JPPIPA 10(4) (2024)

Jurnal Penelitian Pendidikan IPA

Journal of Research in Science Education

http://jppipa.unram.ac.id/index.php/jppipa/index

The Effect of Concentration Transition Metal Oxide CuO as Activated Carbon-Based Supercapacitor

Maryati Doloksaribu[1]*, Erniwati Halawa[1], Mukti Hamjah Harahap[1]

[1] Department of Physics, Universitas Negeri Medan, Medan, Indonesia.

Received: October 18, 2023
Revised: February 22, 2024
Accepted: April 25, 2024
Published: April 30, 2024

Corresponding Author:
Maryati Doloksaribu
maryatidoloksaribu@unimed.ac.id

DOI: 10.29303/jppipa.v10i4.5738

Abstract: Supercapacitors are promising energy storage devices in future energy technology. In this research, the primary and applied aspects of supercapacitors are developed. Various techniques have been developed specifically to estimate specific capacitances. Various attempts have been made in the literature to increase the specific capacitance value of the electrode materials. Electrode materials with unique structural and electrochemical properties, such as high capacity and cyclic stability, exhibit good supercapacitor performance. Many new electrode materials have been developed to play an essential role in capacitance behavior. This research focuses on the highly efficient application of nanostructured electrode materials such as nanoporous carbon and metal oxide CuO for supercapacitors. Nanopore carbon is made from coconut shell, which is synthesized using a simple heating method. Next, carbon nanopore and CuO nanoparticle composites were carried out with composition variations of 0.5,10,15, and 20% of the total weight. The results of cyclic voltammetry, electrochemical impedance spectroscopy, and charge-discharge tests, maximum results were obtained on a composition of 5% CuO nanoparticles with a capacitance of 280 F/gr and a conductivity of 1.14 X 10-2 S/cm. This result is due to an increase in the surface area between the pore surfaces, so more ions are trapped, causing the filling process to take place quickly.

Keywords: CuO; Nanoparticle; Nanoporous; Supercapacitor; Surface area

Introduction

Supercapacitors as energy storage devices have been widely used in the electronics and transportation fields, such as digital telecommunications systems, computers and pulse laser systems, hybrid electrical vehicles, and so on (G.-X. Wang et al., 2005; Y. Wang et al., 2015; Zhu et al., 2007). The latest development of supercapacitors is characterized by the development of electrode material construction with a large surface area and small resistance so that it can increase energy storage capacity. In the charging process, ions will be stored at the electrode and electrolyte interface. This shows that the surface area of the electrode largely determines the energy storage mechanism Therefore, surface area is an important factor that determines load storage capacity. The greater the surface area, the greater the capacitance (Bose et al., 2012; Enock et al., 2017; Nor et al., 2017).

However, despite the high specific surface area, the application of porous carbon materials has been limited to the overall use of the pores for charge accumulation. For activated carbon, from theoretical observations the capacitance is usually only around 10- 20% due to the presence of micropores which are inaccessible to the electrolyte on the electrode surface, so it is unable to form a double layer in the pores (Timperman et al., 2012). Several methods have been used to control the micro and macro structure of porous carbon, but these techniques are difficult and expensive (Candelaria et al., 2012; Frackowiak et al., 2001; Fuertes et al., 2014).

In general, nanoporous carbon produced by researchers (Fernández et al., 2008; Frackowiak et al., 2013; Largeot et al., 2008) has a low mesopore distribution, macropore distribution still appears even though literature studies show that mesopores play a vital role in providing access for electrolyte ions to enter micropores (Fuertes et al., 2014; Lozano-Castelló et al.,

How to Cite:
Doloksaribu, M., Halawa, E., & Harahap, M. H. (2024). The Effect of Concentration Transition Metal Oxide CuO as Activated Carbon-Based Supercapacitor. *Jurnal Penelitian Pendidikan IPA*, *10*(4), 1698–1706. https://doi.org/10.29303/jppipa.v10i4.5738

2002; Qu et al., 1998; Zhuiykov, 2014). To overcome this problem, supercapacitors were developed in a composite structure which is expected to increase the capacitance. Several researchers made nano-porous carbon composites with metal oxide nanoparticles. Metal oxide nanoparticles are used as a substitute because these metal oxides in the form of conductors or semiconductors show active redox properties which produce pseudo capacities (H. Lee et al., 2010; Lu et al., 2011). Metal oxide nanoparticles are promising electrode materials because they can accelerate the reduction and oxidation reactions in the charging and discharging processes, thereby increasing the potential voltage and increasing the charge capacity of the supercapacitor (Etape et al., 2017; Faraji et al., 2014). Pseudocapacitance can increase capacitance significantly because it involves faraday reactions, voltage-dependent between electrodes and electrolytes, either in the form of surface adsorption redox reactions with electrolytes, or doping/undoping of electrode materials (G. Wang et al., 2012). Therefore, it is necessary to conduct research on nanoporous carbon/metal oxide composites to improve supercapacitor performance. Charging and discharging mechanisms in nanoporous carbon composited nanoparticle metal oxide supercapacitors.

The value of the specific capacitance of the supercapacitor can be calculated using the following equation (G. Wang et al., 2012):

$$C_{sp} = \frac{\int Idv}{Smv} \quad (1)$$

Description:

Csp = specific capacitance (F/gr)

(∫Idv)/v = integration of current vs voltage CV curve (Ampere. Volt)

S = Scan rate (mV/s)

m = mass of electrode material (g)

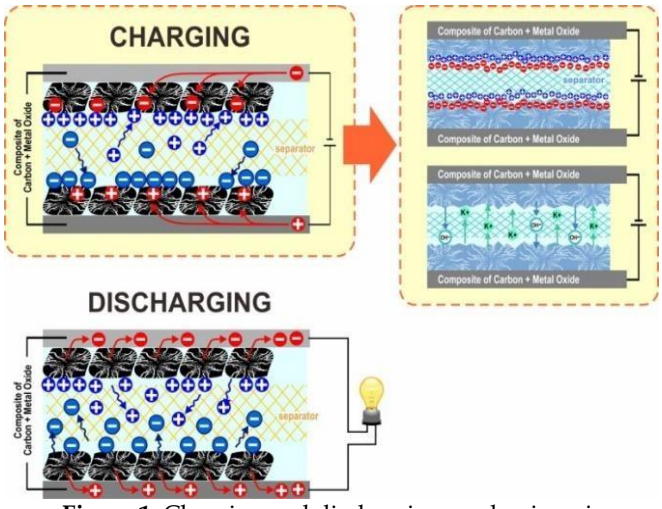

Figure 1. Charging and discharging mechanisms in supercapacitors

Method

This research was conducted in 2 stages, namely the manufacture of nanoporous carbon and nanoporous carbon composited nanoparticle CuO which were assembled into supercapacitor prototypes.

Nanoporous Carbon

The chemical activation process is carried out by mixing carbon charcoal from a coconut shell with KOH (Ajina et al., 2010; Jain et al., 2013; Musa et al., 2015) with a ratio of carbon charcoal and KOH of 1:3. The mixture of carbon and KOH was stirred at a temperature of 90oC by adding distilled water to keep the mixture concentrated. The mixture of KOH and carbon charcoal was left for 24 hours at room temperature and then filtered with filter paper. Furthermore, the filtered carbon was physically activated for 1 hour at various temperatures of 600, 700, and 800°C in a furnace with N2 gas. The carbon powder produced through the activation process is washed with distilled water repeatedly until the pH is normal and to remove the remaining alkaline salts contained in the nanoporous carbon. The washed samples were then filtered and dried at 110°C for 2 hours in a heating oven. Next, surface area, pore size, and morphology tests were carried out using TEM, SEM, and XRD.

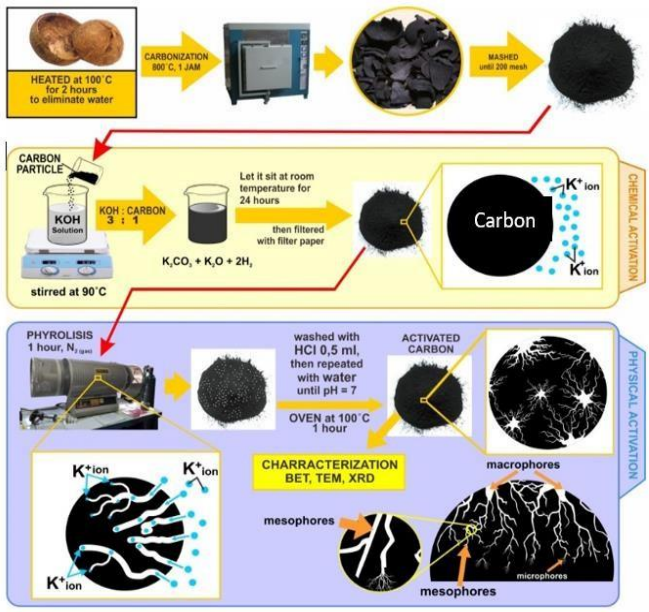

Figure 2. Process nanoporous carbon

Nanoporous Carbon/Metal oxide CuO Composite

Nanoporous carbon composites were carried out on nanoporous carbon with the highest surface area. Composites were made by mixing nanoporous carbon with metal oxides in which the mass percent ratio of metal oxides was CuO (0.5, 10, 15, 20%). The process of mixing nanoporous carbon with metal oxides is carried

out in a beaker glass by adding PVDF binder as much as 10% of the total mass of the material and stirring the DMAC solution for 30 minutes, then adding activated carbon and stirring for 30 minutes, then adding metal oxides according to their respective composition for 2 hours until the mixture is homogeneous and forms slurry (paste). Furthermore, the paste formed was cast on aluminum foil using the Doctor Blade method, after that it was baked in the oven at 80°C for 30 minutes, then in a vacuum oven for 12 hours to remove the gas in the pores and then cut into coin pellets and assembled. Supercapacitors are composed of two electrodes, a separator, and an electrolyte. Both electrodes are made from nanoporous composite materials and metal oxide nanoparticles. The electrode is made in the shape of a circle with a diameter of 16 mm. The separator and electrolyte used in this research were polypropylene and 3M KOH in distilled water (Akinwolemiwa et al., 2015). Supercapacitor assembly process using a coin cell consisting of a base, cover, and spacer. First, the cell coins are washed using acetone and then dried in a vacuum oven at 70 °C for 30 minutes. Furthermore, the coin cell components, electrodes, separators, electrolytes, and spacers are arranged in a row as follows: base, electrodes as shown in Figure 3. After the assembly process is complete, the supercapacitor fabrication can be said to have been successful, Next is the Cyclic Voltammetry (CV) test, Charge-Discharge (CD), and Electrochemical impedance spectroscopy (EIS) using the WBCS 3000, SEM mapping testing to determine the distribution of metal oxides and XRD tests to determine the structure formed by the composite.

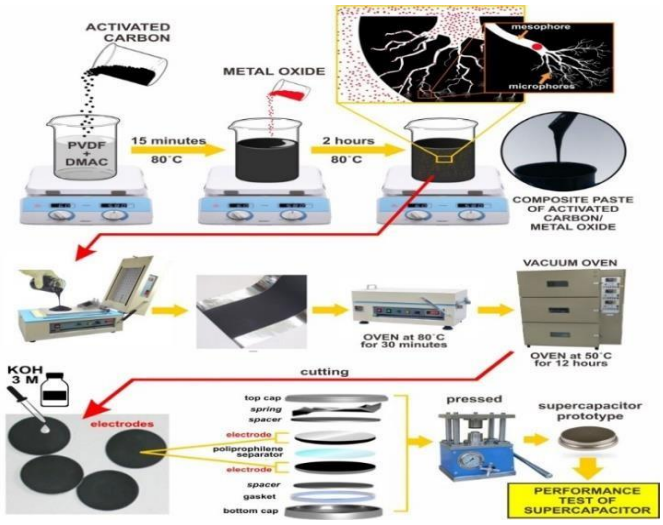

Figure 3. Composite nanoporous carbon and metal oxide

Result and Discussion

Nanoporous Carbon

Nitrogen physisorption isotherm characterization of nanoporous carbon activated for 1 hour with temperature variations of 600°C, 700°C, and 800°C. From this characterization, surface area and pore size distribution can be derived.

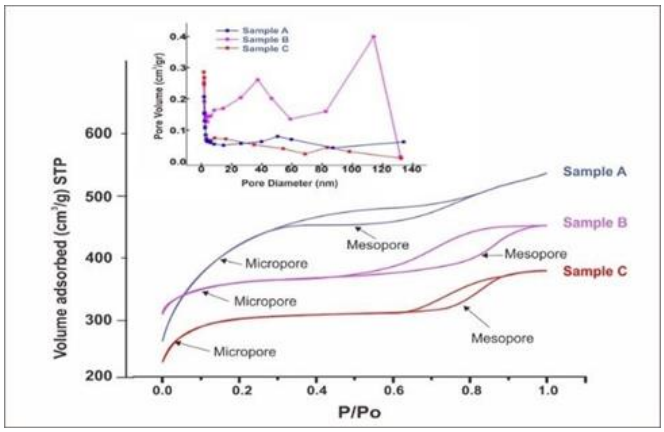

Figure 4. Nitrogen physisorption isotherm and pore diameter of Nanoporous carbon

Samples have a high specific surface area (above 1,000 m^2/g). With the simple heating method, obtaining a high surface area can be done quickly and economically. According to Qu et al. (1998), materials with a surface area of more than 1000 m^2/g are suitable for application as electrodes in supercapacitors. The specific surface area measured by the BET method or known as SBET shows an increase with the increase in activation time for carbon nanoporous samples activated at a temperature of 700°C but at a temperature of 800°C, there is a decrease in the surface area due to pore widening due to an increase in temperature so that the number of pores in the macroporous phase increases. increasing (Barranco et al., 2010; Kierzek et al., 2004; Li et al., 2013).

Figure 4 is the absorption-desorption isotherm curve of nanoporous carbon produced at temperatures of 600 °C, 700 °C, and 800 °C for 60 minutes. Samples labeled A, B, and C are nanoporous carbon which represents type I physisorption isotherm adsorption or what is known as Langmuir. Where the sample still has micropores with a narrow external surface. In sample B the isotherm curve looks sharp, with a larger adsorption volume, this shows a widening of the pore size as N2 adsorption increases. The hysteresis curves in samples A, B, and C show a slight H4-type hysteresis loop which indicates that the material has slit-pore-shaped pores (Burke et al., 2014; Sing, 1982). This indicates the presence of more mesopores as also found by Yang et al. (2008). H4 hysteresis shows unlimited adsorption at high relative pressures Hu et al. (2001) finding materials with H4-type loops resembling plate-like aggregates that are larger than slit-shaped pores. The isotherm curve characteristics for samples A and C appear to have decreased for nitrogen adsorption. Figure 5 shows the size of the pore diameter in carbon A, B, and C. It can be

seen that carbon A, B, and C still have pores at macro size even though the surface area is high.

Table 1. Physical Characteristics of Nanoporous Carbon

Code	Temp ^{0}C	Surface area (m^2/g)	Average pore diameter (nm)	Total pore volume (cc/g)
A	600	1089	12.50	0.68
B	700	1469	11.60	0.85
C	800	1056	15.20	0.80

Figure 5 shows the TEM and FESEM characteristics of activated carbon with a surface area of 1469 m^2/g. It appears that the majority of pore sizes are in the mesoporous phase (2-50 nm) and appear to still be present in macropore sizes (> 50 nm). This result is in accordance with the pore diameter graph. generated by BJH BET data.

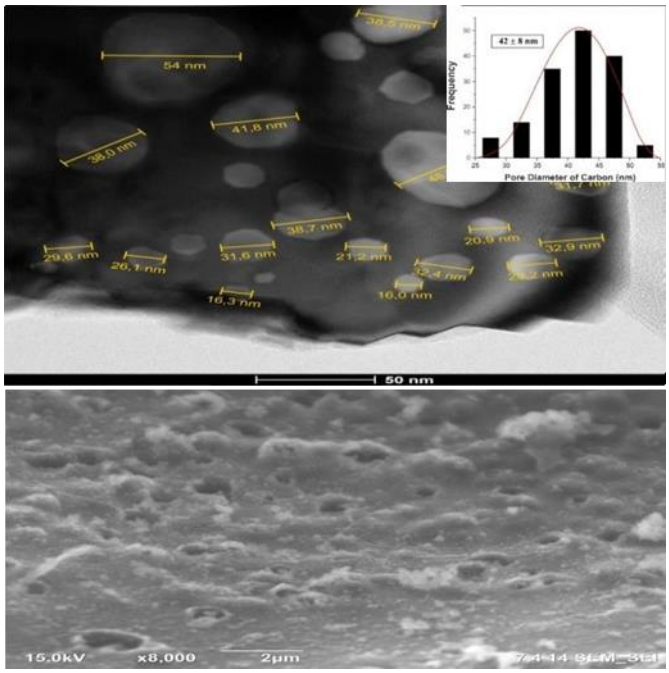

Figure 5. TEM and FESEM pore distribution of nanoporous carbon

Figure 6 is the XRD profile of the result nanoporous carbon. The results of x-ray diffraction (ʎ = 1.54Å) show 2 carbon peaks at an angle of 2θ, each at 23.5^o and 44^o. The diffraction angle value corresponds to the miller carbon index (002), (101). Nanoporous carbon has a (002) reflection between 20^o and 30^o indicating the presence of coherent graphene stacks and parallel in a limited domain (Hwang et al., 2008). Wave peak with FWHM of 11.4^o and lattice spacing (002) of 3.4 Å. This shows that the structure of nanoporous carbon becomes more regular, namely approaching the structure of graphite with a lattice spacing of 3.4 Å (Fey et al., 2003). Distance the lattice that gets closer to graphite shows a decrease in the amorphous part which is the location for the formation of smaller pores. In addition, at a diffraction angle of 2θ between 40^o and 50^o a clearer peak is visible. This peak shows carbon with a (101) orientation which indicates a hexagonal structure (Hwang et al., 2008).

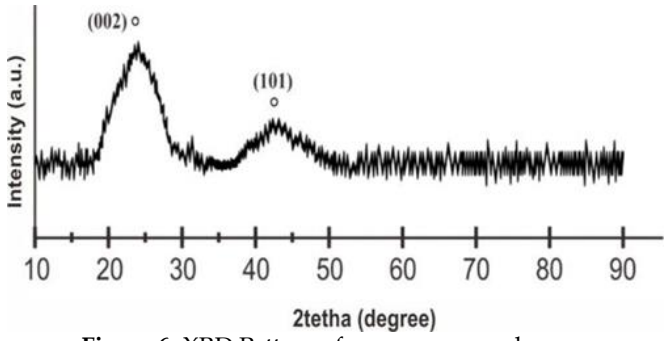

Figure 6. XRD Pattern of nanoporous carbon

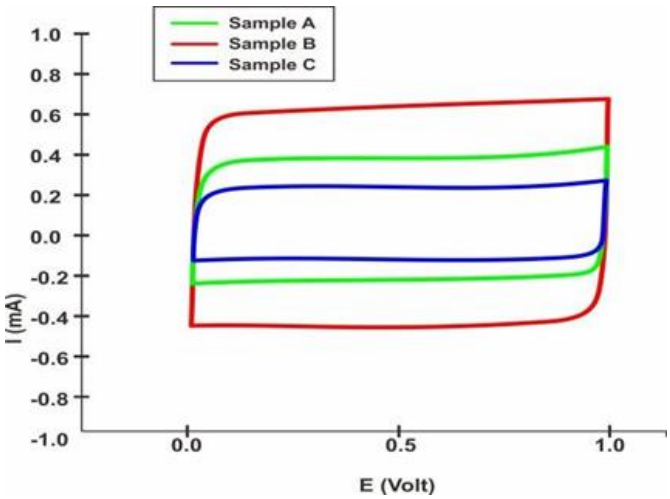

Figure 7. Cyclic voltammetry profile of nanoporous carbon at 10 mv/S

Figure 7 electrochemical performance of nanoporous carbon-based supercapacitors obtained by cyclic voltammetry characterization with a scan rate of 10 mV/s. The capacitance for nanoporous carbon samples A, B, and C measured based on Equation (1) with an electrode mass of 0.002 g is 80.9 F/g, 100 F/g, 135 F/g, and 78.7 F/g. Of all the samples, the capacitance of sample B has the maximum value due to the large pore size distribution in the mesopore class. Apart from that, this is possible with the presence of crystal orientation which can increase electrical conductivity (Beguin, 2009; G.-J. Lee et al., 2007; Pandolfo et al., 2006).

From this EIS measurement, cell conductivity can be calculated where the thickness of the sample material is 0.01 cm, and the sample area is 2 cm^2. From the calculation results, the conductivity of sample A = 3 x 10-04 S/cm, sample B = 3.5 x 10-04 S/cm, and sample C = 2.89 x 10-04 S/cm with RA = 41, 5 ohms, RB = 36 ohms, RC = 87.5 ohms. From these results, it can be seen that the smallest resistance is in sample B with a resistance value of 36 ohms. Small resistance indicates fast ion transport and low power dissipation. Therefore, in the

nanopore activated carbon composite process with CuO nanoparticles used is sample B.

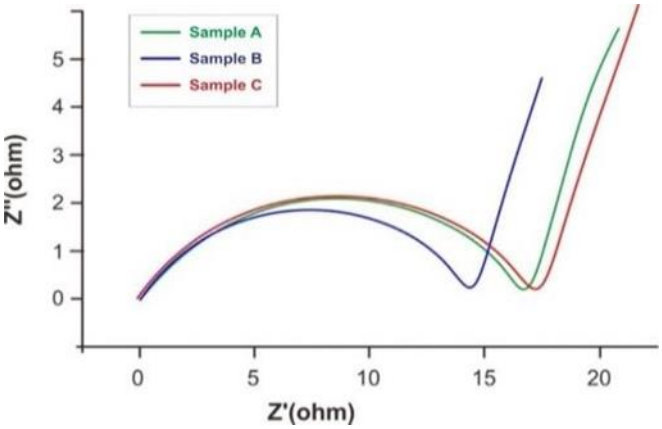

Figure 8. Electrochemical impedance spectroscopy of nanoporous activated carbon samples A, B, C.

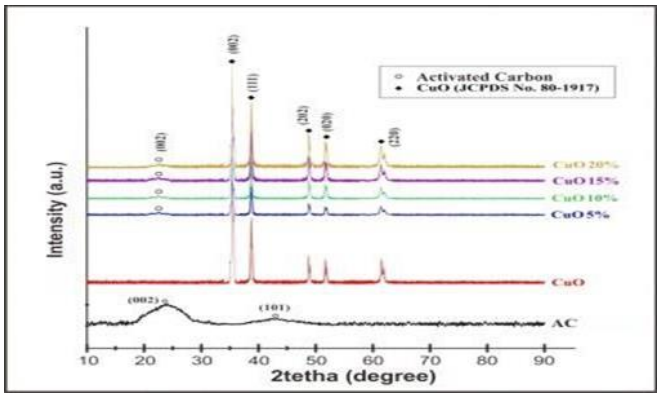

Figure 9. XRD profile of nanoporous carbon composite/CuO nanoparticles

Figure 9 is the XRD spectrum of nanoporous activated carbon, CuO nanoparticles. The CuO peaks are at angles 2θ (35.43), (38.90), (48.83), (53.60), (61.59) on the (002), (111), (200), (202), (020), and (220). From this pattern, it can be seen that there is no change in the crystal structure and changes in the crystal lattice spacing of the nanoporous activated carbon due to the addition of metal oxide. Diffraction peaks of nanoporous activated carbon and metal oxide CuO still appear in the composite electrode material. This concludes that there is no reaction due to the addition of CuO metal oxide nanoparticles. The properties of composited nanoporous carbon/metal oxide are a combination of the physical and chemical properties of metal oxide and carbon nanoparticles. In this composite, only interfacial bonding occurs between metal oxide and carbon nanoparticles and there is no compound (Figure 10).

Figure 10 is TEM data which includes Selected Area Electron Diffraction (SAED) data. SAED data indicates that the nanoporous activated carbon/CuO nanoparticle composite is single-crystalline with sample planes obtained (002), (111), (202), (020), and (220). From the TEM image it can also be calculated that the grain diameter of the nanoporous carbon/CuO nanoparticle composite is around 30 nm.

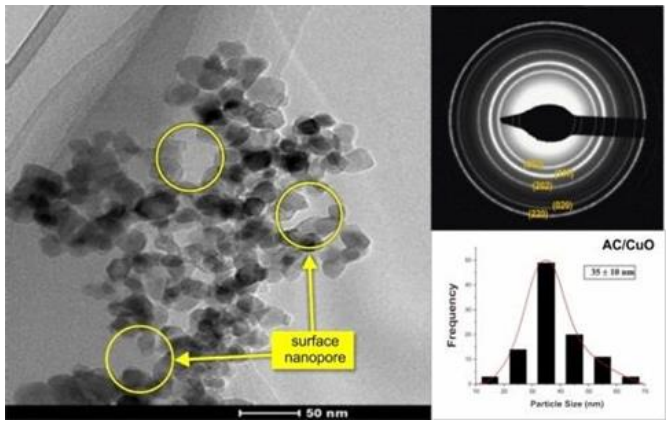

Figure 10. TEM spectra of nanopore carbon/CuO nanoparticles

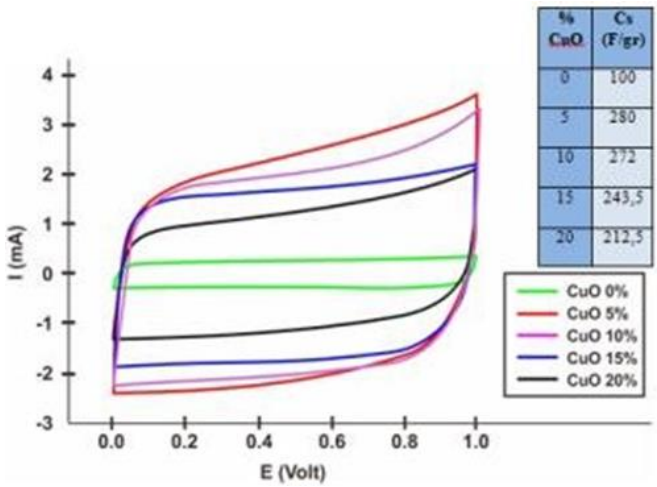

Figure 11. Cyclic voltammetry profile of nanoporous carbon/metal oxide

In the performance test of the nanoporous activated carbon supercapacitor used was nanoporous activated carbon with the highest surface area, 1469 m^2/g with the aim of obtaining a higher capacitance. Figure 5.34 is a cyclic voltammetry curve with a scan rate of 10 mV/s and a sample mass of 0.002 gr. The amount of capacitance can be calculated using Equation (1). The specific capacitance values are 100 F/g, 280 F/g, 190.80 F/g, 146 F/g, and 116.6 F/g for samples 0% CuO, 5%CuO, and 10% CuO, respectively. 15% CuO and 20% CuO. The energy that can be stored/kg is 13.89 J, 38.89 J, 37.78 J, 33.82 J, 29.51 J, and power that can be stored/kg is 0.002 W, 0.022 W, 0.006 W, 0.002 W, 0.001 W for each sample of 0% CuO, 5% CuO, 10% CuO, 15% CuO, and 20% CuO. The performance of the 5% CuO sample which produces maximum capacitance is caused by the pore size distribution in the mesoporous class. From the overall capacitance results, it can be seen that the specific surface area is proportional to the resulting capacitance

as seen in the 5% CuO sample which has a maximum specific surface area that is better than Zhang et al. (2013).

The presence of metal oxide CuO nanoparticles functions to increase the capacitance value of the supercapacitor through redox reactions on the electrode surface. inside the supercapacitor and increases the dielectricity value of the supercapacitor (Park et al., 2002; S. Wang et al., 2017; Wu et al., 2012; J. Zhang et al., 2012). Remembering that the amount of energy stored in a supercapacitor depends on the amount of ions are stored, then the oxidation state in the CuO crystal structure will contribute to increasing the capacitance. In the cyclic voltammetry test, it appears that the more CuO composition is added, the capacitance value decreases, this is because the number of added nanoparticles covers the pores in the composite, causing the surface area to decrease, resulting in a decrease in the capacitance value. The charge storage mechanism that occurs on the electrode surface which is a nanoporous carbon/CuO composite is:

$$(CuO)_{surface} + K^{+} + OH^{-} \leftrightarrow (CuOK^{+}OH^{-})_{surface} \quad (2)$$

Figure 12 is the result of the charge discharge test which shows the relationship between the length of charging and discharging time when a load current of 1A is applied. From the picture it can be learned that the supercapacitor cell is capable of having basic properties as an electrical energy storage device, characterized by two characteristics, namely a decrease in current with the passage of charging time and the cell is able to withstand the characteristic voltage level of a supercapacitor cell.

The voltage achieved is very good because it is close to the standard voltage value for KOH electrolyte = 1 volt (distilled water base). During the charging process, the charge occurs to a potential of 1 volt. From the picture it appears that the charging and discharging times for each electrode are different. At 0% CuO charging time 350 seconds discharging 450 seconds, 5% CuO charging 1800 seconds discharging 2750 seconds, 10% CuO charging time 1800 seconds discharging 2000 seconds, 15% CuO charging time 1800 seconds discharging 1800 seconds and 20% CuO charging time 1800 blanking seconds 1000 seconds. It appears that at 5% CuO, the discharge time is longer because more ions are stored due to the high surface area. During the discharging process, the voltage will decrease further due to loss of charge, and the voltage never rises again to a reference potential. This decrease shows the cell's ability to fill. However, the cell's discharging capability is still very low because it can only draw a current of no more than 1A and the cell voltage immediately drops drastically to 0V. From the test results it still appears that the charging and discharging capabilities of supercapacitor cells are the same, however, this cell can still be considered as a supercapacitor cell because its capacitance is still promising.

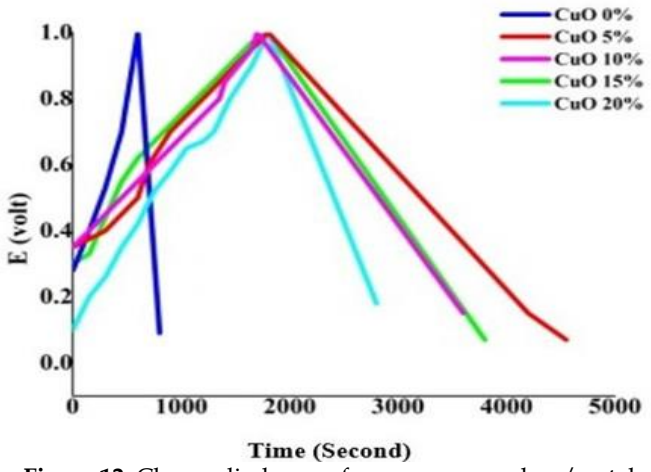

Figure 12. Charge discharge of nanoporous carbon/metal oxide

Conductivity measurements were carried out using the EIS (Electrochemical Impedance Spectroscopy) method (Figure 13). The EIS curve has formed properly. A good electrode will form a semicircle pattern. Impedance measurements are carried out by applying a DC bias voltage of 1V. The frequency spectrum range is given between 4 Hz - 1 MHz. From this EIS measurement, cell conductivity can be calculated using a material resistivity equation. From the calculation results, the conductivity of 0% CuO is 3.55 x 10-04 S/cm, 5% CuO 1.14 x 10-02 S/cm, 10% CuO 1.52 x 10-03 S/cm, 15% CuO 7.79 x 10-04 S/cm, 20% CuO 5.77 x 10-04 S/cm. From these results, it can be seen that the highest conductivity is at the 5% CuO position with a resistance of 3.2 ohms. Small resistance indicates fast ion transport. From the overall results, the highest capacitance was in the 5% metal oxide composite, this result was because this composition had a high surface area and the pore size was in the mesoporous phase.

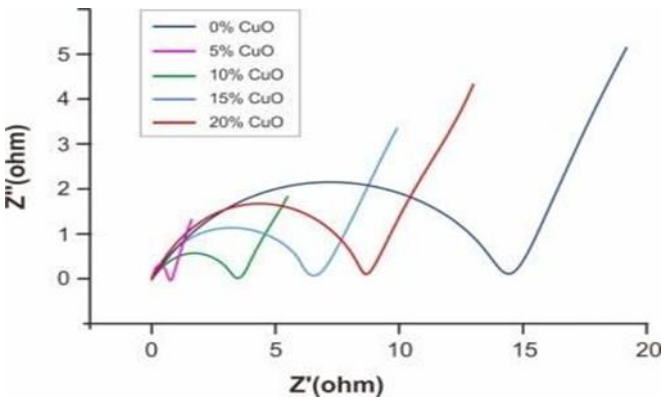

Figure 13. EIS profile Nanoporous carbon/CuO Nanoparticle

Conclusion

Conclusions on the results and discussion of the series of research results above are as follows: The addition of metal oxide nanoparticles to the surface of nanoporous activated carbon can increase the capacitance almost twice when compared to supercapacitors that use nanoporous activated carbon alone. The addition of 5% CuO maximum capacitance of 280 F/g. Supercapacitors based on nanoporous carbon/transition metal oxide nanoparticle composites reduce the average pore diameter in the range of 40 nm-60 nm. So the dominant pore size is in the mesoporous fraction and increases the specific surface area, mesopore surface area, and pore volume.

Acknowledgments
Thanks are expressed to the Chancellor and Chair of the Institute for Research and Community Service who have provided funding from the 2023 PNBP with contract number 0008/UN 33.8/KPT/PPT/2023, as well as other related parties who have supported this research until it was completed.

Author Contributions
Conceptualization, methodology, formal analysis, writing original draft, MD; supervision, resources, project administration, EH; writing—review and editing, project administration, validation, MJH. All authors have read and agreed to the published version of the manuscript.

Funding
This research was funded by PNBP UNIMED. The author(s) received financial support for the research, authorship, and/or publication of this article.

Conflicts of Interest
No conflict interest.

References

Ajina, A., & Isa, D. (2010). Symmetrical Supercapacitor Using Coconut Shell-Based Activated Carbon. *Pertanika Journal of Science and Technology*, *18*(2), 351–363. Retrieved from https://rb.gy/kv6jd1

Akinwolemiwa, B., Peng, C., & Chen, G. Z. (2015). Redox Electrolytes in Supercapacitors. *Journal of The Electrochemical Society*, *162*(5), A5054–A5059. https://doi.org/10.1149/2.0111505jes

Barranco, V., Lillo-Rodenas, M. A., Linares-Solano, A., Oya, A., Pico, F., Ibañez, J., Agullo-Rueda, F., Amarilla, J. M., & Rojo, J. M. (2010). Amorphous Carbon Nanofibers and Their Activated Carbon Nanofibers as Supercapacitor Electrodes. *The Journal of Physical Chemistry C*, *114*(22), 10302–10307. https://doi.org/10.1021/jp1021278

Beguin, F. (2009). *Electrical Double-Layer Capacitors and Pseudocapacitors From Carbons for Electrochemical Energy Storage and Conversion Systems*. CRC Press.

Bose, S., Kuila, T., Mishra, A. K., Rajasekar, R., Kim, N. H., & Lee, J. H. (2012). Carbon-based nanostructured materials and their composites as supercapacitor electrodes. *Journal of Materials Chemistry*, *22*(3), 767–784. https://doi.org/10.1039/c1jm14468e

Burke, A., Liu, Z., & Zhao, H. (2014). Present and future applications of supercapacitors in electric and hybrid vehicles. *2014 IEEE International Electric Vehicle Conference, IEVC 2014*. https://doi.org/10.1109/IEVC.2014.7056094

Candelaria, S. L., Garcia, B. B., Liu, D., & Cao, G. (2012). Nitrogen modification of highly porous carbon for improved supercapacitor performance. *Journal of Materials Chemistry*, *22*(19), 9884. https://doi.org/10.1039/c2jm30923h

Enock, T. K., King'ondu, C. K., Pogrebnoi, A., & Jande, Y. A. C. (2017). Status of Biomass Derived Carbon Materials for Supercapacitor Application. *International Journal of Electrochemistry*, *2017*, 1–14. https://doi.org/10.1155/2017/6453420

Etape, E. P., John Ngolui, L., Foba-Tendo, J., Yufanyi, D. M., & Victorine Namondo, B. (2017). Synthesis and Characterization of CuO, TiO 2 , and CuO-TiO 2 Mixed Oxide by a Modified Oxalate Route. *Journal of Applied Chemistry*, *2017*, 1–10. https://doi.org/10.1155/2017/4518654

Faraji, S., & Ani, F. N. (2014). Microwave-assisted synthesis of metal oxide/hydroxide composite electrodes for high power supercapacitors – A review. *Journal of Power Sources*, *263*, 338–360. https://doi.org/10.1016/j.jpowsour.2014.03.144

Fernández, J. A., Arulepp, M., Leis, J., Stoeckli, F., & Centeno, T. A. (2008). EDLC performance of carbide-derived carbons in aprotic and acidic electrolytes. *Electrochimica Acta*, *53*(24), 7111–7116. https://doi.org/10.1016/j.electacta.2008.05.028

Fey, G. T. K., Lee, D. C., Lin, Y. Y., & Prem Kumar, T. (2003). High-capacity disordered carbons derived from peanut shells as lithium-intercalating anode materials. *Synthetic Metals*, *139*(1), 71–80. https://doi.org/10.1016/S0379-6779(03)00082-1

Frackowiak, E., Abbas, Q., & Béguin, F. (2013). Carbon/carbon supercapacitors. *Journal of Energy Chemistry*, *22*(2), 226–240. https://doi.org/10.1016/S2095-4956(13)60028-5

Frackowiak, E., & Béguin, F. (2001). Carbon materials for the electrochemical storage of energy in capacitors. *Carbon*, *39*(6), 937–950. https://doi.org/10.1016/S0008-6223(00)00183-4

Fuertes, A. B., Ferrero, G. A., & Sevilla, M. (2014). One-pot synthesis of microporous carbons highly enriched in nitrogen and their electrochemical performance. *J. Mater. Chem. A*, *2*(35), 14439–14448.

https://doi.org/10.1039/C4TA02959C

Hwang, Y. J., Jeong, S. K., Shin, J. S., Nahm, K. S., & Stephan, A. M. (2008). High capacity disordered carbons obtained from coconut shells as anode materials for lithium batteries. *Journal of Alloys and Compounds*, *448*(1-2), 141–147. https://doi.org/10.1016/j.jallcom.2006.10.036

Jain, A., Aravindan, V., Jayaraman, S., Kumar, P. S., Balasubramanian, R., Ramakrishna, S., Madhavi, S., & Srinivasan, M. P. (2013). Activated carbons derived from coconut shells as high energy density cathode material for Li-ion capacitors. *Scientific Reports*, *3*(1), 3002. https://doi.org/10.1038/srep03002

Kierzek, K., Frackowiak, E., Lota, G., Gryglewicz, G., & Machnikowski, J. (2004). Electrochemical capacitors based on highly porous carbons prepared by KOH activation. *Electrochimica Acta*, *49*(4), 515–523. https://doi.org/10.1016/j.electacta.2003.08.026

Largeot, C., Portet, C., Chmiola, J., Taberna, P.-L., Gogotsi, Y., & Simon, P. (2008). Relation between the Ion Size and Pore Size for an Electric Double-Layer Capacitor. *Journal of the American Chemical Society*, *130*(9), 2730–2731. https://doi.org/10.1021/ja7106178

Lee, G.-J., & Pyun, S.-I. (2007). *Synthesis and Characterization of Nanoporous Carbon and its Electrochemical Application to Electrode Material for Supercapacitors*. Springer: Modern Aspects of Electrochemistry. https://doi.org/10.1007/978-0-387-46108-3_2

Lee, H., Cho, M. S., Kim, I. H., Nam, J. Do, & Lee, Y. (2010). RuOx/polypyrrole nanocomposite electrode for electrochemical capacitors. *Synthetic Metals*, *160*(9-10), 1055–1059. https://doi.org/10.1016/j.synthmet.2010.02.026

Li, B., Gao, G., Zhai, D., Wei, C., He, Y., Du, H., & Kang, F. (2013). Synthesis, characterization and electrochemical performance of manganese dioxide in a quaternary microemulsion: The role of the co-surfactant and water. *International Journal of Electrochemical Science*, *8*(6), 8740–8751. https://doi.org/10.1016/s1452-3981(23)12924-5

Lozano-Castelló, D., Alcañiz-Monge, J., de la Casa-Lillo, M. ., Cazorla-Amorós, D., & Linares-Solano, A. (2002). Advances in the study of methane storage in porous carbonaceous materials. *Fuel*, *81*(14), 1777–1803. https://doi.org/10.1016/S0016-2361(02)00124-2

Lu, W., Hartman, R., Qu, L., & Dai, L. (2011). Nanocomposite electrodes for high-performance supercapacitors. *Journal of Physical Chemistry Letters*, *2*(6), 655–660. https://doi.org/10.1021/jz200104n

Musa, M. S., Sanagi, M. M., Nur, H., & Wan Ibrahim, W. A. (2015). Understanding Pore Formation and Structural Deformation in Carbon Spheres During KOH Activation. *Sains Malaysiana*, *44*(4), 613–618. https://doi.org/10.17576/jsm-2015-4404-17

Nor, N. S. M., Deraman, M. S., Suleman, M., Jasni, M. R. M., Manjunatha, J. G., Othman, M. A. R., & Shamsudin, S. A. (2017). Supercapacitors using Binderless Activated Carbon Monoliths Electrodes consisting of a Graphite Additive and Pre-carbonized Biomass Fibers. *International Journal of Electrochemical Science*, *12*(3), 2520–2539. https://doi.org/10.20964/2017.03.48

Pandolfo, A. G., & Hollenkamp, A. F. (2006). Carbon properties and their role in supercapacitors. *Journal of Power Sources*, *157*(1), 11–27. https://doi.org/10.1016/j.jpowsour.2006.02.065

Park, J. H., & Park, O. O. (2002). Hybrid electrochemical capacitors based on polyaniline and activated carbon electrodes. *Journal of Power Sources*, *111*(1), 185–190. https://doi.org/10.1016/S0378-7753(02)00304-X

Qu, D., & Shi, H. (1998). Studies of activated carbons used in double-layer capacitors. *Journal of Power Sources*, *74*(1), 99–107. https://doi.org/10.1016/S0378-7753(98)00038-X

Sing, K. S. W. (1982). Reporting physisorption data for gas/solid systems. *Pure and Applied Chemistry*, *54*(11), 2201–2218. https://doi.org/10.1351/pac198254112201

Timperman, L., Skowron, P., Boisset, A., Galiano, H., Lemordant, D., Frackowiak, E., Béguin, F., & Anouti, M. (2012). Triethylammonium bis(tetrafluoromethylsulfonyl)amide protic ionic liquid as an electrolyte for electrical double-layer capacitors. *Physical Chemistry Chemical Physics*, *14*(22), 8199. https://doi.org/10.1039/c2cp40315c

Wang, G., Zhang, L., & Zhang, J. (2012). A review of electrode materials for electrochemical supercapacitors. *Chem. Soc. Rev.*, *41*(2), 797–828. https://doi.org/10.1039/C1CS15060J

Wang, G.-X., Zhang, B.-L., Yu, Z.-L., & Qu, M.-Z. (2005). Manganese oxide/MWNTs composite electrodes for supercapacitors. *Solid State Ionics*, *176*(11-12), 1169–1174. https://doi.org/10.1016/j.ssi.2005.02.005

Wang, S., Wang, R., Zhang, Y., & Zhang, L. (2017). Highly porous carbon with large electrochemical ion absorption capability for high-performance supercapacitors and ion capacitors. *Nanotechnology*, *28*(44), 445406. https://doi.org/10.1088/1361-6528/aa848a

Wang, Y., Guo, J., Wang, T., Shao, J., Wang, D., & Yang, Y.-W. (2015). Mesoporous Transition Metal Oxides for Supercapacitors. *Nanomaterials*, *5*(4), 1667–1689.

https://doi.org/10.3390/nano5041667

Wu, Z. S., Zhou, G., Yin, L. C., Ren, W., Li, F., & Cheng, H. M. (2012). Graphene/metal oxide composite electrode materials for energy storage. *Nano Energy*, *1*(1), 107–131. https://doi.org/10.1016/j.nanoen.2011.11.001

Yang, J., Liu, Y., Chen, X., Hu, Z., & Zhao, G. (2008). Carbon Electrode Material with High Densities of Energy and Power. *Acta Physico - Chimica Sinica*, *24*(1), 13–19. https://doi.org/10.1016/S1872-1508(08)60002-9

Zhang, J., & Zhao, X. S. (2012). On the Configuration of Supercapacitors for Maximizing Electrochemical Performance. *ChemSusChem*, *5*(5), 818–841. https://doi.org/10.1002/cssc.201100571

Zhang, L., Candelaria, S. L., Tian, J., Li, Y., Huang, Y. X., & Cao, G. (2013). Copper nanocrystal modified activated carbon for supercapacitors with enhanced volumetric energy and power density. *Journal of Power Sources*, *236*, 215–223. https://doi.org/10.1016/j.jpowsour.2013.02.036

Zhu, Y., Hu, H., Li, W., & Zhang, X. (2007). Resorcinol-formaldehyde based porous carbon as an electrode material for supercapacitors. *Carbon*, *45*(1), 160–165. https://doi.org/10.1016/j.carbon.2006.07.010

Zhuiykov, S. (2014). *Nanostructured Semiconductor Oxides for the Next Generation of Electronics and Functional Devices*. Woodhead Publishing.